Computational Materials Science 48 (2010) 730–735

Contents lists available at ScienceDirect

Computational Materials Science

journal homepage: www.elsevier.com/locate/commatsci

A molecular mechanics approach for the vibration of single-walled carbon nanotubes

R. Chowdhury [a,*], S. Adhikari [a], C.Y. Wang [a], F. Scarpa [b]

[a] Multidisciplinary Nanotechnology Centre, Swansea University, Singleton Park, Swansea SA2 8PP, UK
[b] Advanced Composites Centre for Innovation and Science, University of Bristol, Bristol BS8 1TR, UK

ARTICLE INFO

Article history:
Received 29 January 2010
Received in revised form 9 March 2010
Accepted 15 March 2010
Available online 10 April 2010

Keywords:
Vibrational analysis
Carbon nanotube
Molecular mechanics
Natural frequency
Mode shape

ABSTRACT

We investigate the vibrational properties of zigzag and armchair single-wall carbon nanotubes (CNTs) using the molecular mechanics approach. The natural frequencies of vibration and their associated intrinsic vibration modes are obtained. The simulations are carried out for four types of zigzag nanotubes (5, 0), (6, 0), (8, 0), (10, 0) and three types of armchair nanotubes (3, 3), (4, 4), (6, 6). The universal force field potential is used for the molecular mechanics approach. The first five natural frequencies are obtained for aspect ratios ranging from 5 to 20. The results indicate that the natural frequencies decrease as the aspect ratios increase. The results follow similar trends with results of previous studies for CNTs using structural mechanics approach.

1. Introduction

The discovery of carbon nanotubes (CNTs) [1] has inspired extensive studies on their exceptional mechanical properties [2,3] and potential applications in nanotechnology [4,5]. It has been shown that CNTs with extremely high elastic modulus and low mass density can serve as terahertz nanoresonators [6–9] in nanoelectronics, nanodevices and nanoelectricmechanical systems (NEMS). Specifically, particular vibration modes, e.g., radial breathing mode [10–14], transverse mode [15] and longitudinal mode [16], offer valuable probes for the atomic structures and the elastic properties of CNTs. On the other hand, the vibration of CNTs usually alters the geometry of originally straight single-wall CNTs (SWCNTs) with circular cross-sections, and the concentric structures of multiwall CNTs (MWCNTs). Such deformation could result in sudden changes of the electrical properties of CNTs that are sensitive to their geometrical symmetry [17]. In addition, the oscillation of carbon atoms could also impair the mechanical integrity of CNTs, and lead to the uncertainty of their positions. These in turn will impose significant impacts on the proper functioning of CNT-based nanoelectronics/devices and NEMS. Thus, similar to the buckling behavior [3] the vibration of CNTs remains a major topic of great interest in nanomechanics [2,6–9].

In the last two decades, experimental techniques [10–14,18], atomistic simulations [6,7,9,19–24] and continuum mechanics theories [8,25–29] have been used to predict the phonon dispersion relation [18–22], capture the vibration deformation patterns [27,28] and quantify the dependence of the vibration frequency on the geometrical size [11,12] and molecular structures [26] of CNTs. These studies, however, are primarily focused on MWCNTs. The vibration analysis of SWCNTs is mainly focused on the fundamental mode [6], and Raman active modes including the radial breathing mode and tangential mode [10–13]. To the best of our knowledge, the comprehensive study and profound understanding of the general vibration behavior of SWCNTS as cylindrical structures have not been studied in details. In particular it is well known that SWCNTs possess various atomic structures, i.e., armchair, chiral and zigzag, whose chiral angle rises from zero to 30° [30]. Up till now the effect of such atomic structures on the vibration behavior of SWCNTs has not received enough attention except for a recent study of zigzag tubes based on molecular mechanics (MM) model [31] and a few early studies on the radial breathing modes [13,14].

Under these circumstances the present paper aims to fill the vacancy in this specific area by calculating the general vibration spectra of SWCNTs with armchair and zigzag structures, and various radii and the length-to-diameter aspect ratios. The associated vibration modes will also be captured for SWCNTs and used to understand the dependence of their frequencies on the geometric size of SWCNTs. Here the particular attention will be given to the effect of the atomic structures on the vibration of SWCNTs. The investigation on this issue is of particular interest as the continuum

* Corresponding author. Tel.: +44 (0)1792 602088; fax: +44 (0)1792 295676.
E-mail addresses: R.Chowdhury@swansea.ac.uk (R. Chowdhury), S.Adhikari@swansea.ac.uk (S. Adhikari), Chengyuan.Wang@Swansea.ac.uk (C.Y. Wang), F.Scarpa@bris.ac.uk (F. Scarpa).

0927-0256/$ - see front matter © 2010 Elsevier B.V. All rights reserved.
doi:10.1016/j.commatsci.2010.03.020

models ignoring the atomic details have been employed in the vibration analyses of SWCNTs. To achieve these goals, an MM model which accounts for the atomic structures of SWCNTs is developed and utilized to perform the vibration analysis of SWCNTs. The paper is organized in the following way. Section 2 will be centered on the development and validation of the MM model. The numerical results and discussion will be presented in Section 3. Finally, the major conclusions of this paper will be drawn in Section 4 based on the results and analyses in Section 3.

2. Brief overview of the molecular mechanics approach

From the viewpoint of molecular mechanics, the general expression of total energy is a sum of energies due to valence or bonded interactions and non-bonded interactions

$$E = \sum E_R + \sum E_\theta + \sum E_\phi + \sum E_\omega + \sum E_{VDW} + \sum E_{el} \tag{1}$$

The valence interactions consist of bond stretching (E_R) and angular distortions. The angular distortions are bond angle bending (E_θ), dihedral angle torsion (E_ϕ) and inversion terms (E_ω). The non-bonded interactions consist of van der Waals (E_{VDW}) and electrostatic (E_{el}) terms. In this study, we used universal force field (UFF) model [32], wherein the force field parameters are estimated using general rules based only on the element, its hybridization and its connectivity. The force field functional forms and parameters used in this study are in accordance with Rappe et al. [32].

2.1. Optimization of the CNTs

The optimized equilibrium configurations of the zigzag $(n,0)$ CNTs with $n = 5,6,8$ and 10, and the armchair (n,n) CNTs with $n = 3,4$ and 6, are considered in this vibration analysis. The geometry optimizations were performed with nanotubes. The optimized bond length of C–C and average bond angle of $\angle$C–C is tabulated in Tables 1 and 2, respectively. A small variation in these quantities can be seen in these two tables. Such variations, normally ignored in structural mechanics and continuum mechanics approach, are taken into account in the proposed approach.

2.2. Calculation of the natural frequencies

We start with the Hessian matrix $\mathbf{f}_{\mathrm{CAR}}$, which holds the second partial derivatives of the potential E with respect to the displacement of the atoms in Cartesian coordinates (CAR) [33,34]:

$$f_{\mathrm{CAR}_{ij}} = \left(\frac{\partial^2 E}{\partial \xi_i \partial \xi_j}\right)_{Opt} \tag{2}$$

This is a $3N \times 3N$ matrix (N is the number of atoms), where $\xi_1, \xi_2, \xi_3, \ldots, \xi_{3N}$ are used for the displacements in Cartesian coordinates, $\Delta x_1, \Delta y_1, \Delta z_1, \ldots, \Delta z_N$. The $()_{Opt}$ refers to the fact that the derivatives are taken at the equilibrium positions of the atoms. These force constants are then converted to mass weighted Cartesian coordinates (MWC) [33]

$$f_{\mathrm{MWC}_{ij}} = \frac{f_{\mathrm{CAR}_{ij}}}{\sqrt{m_i m_j}} = \left(\frac{\partial^2 E}{\partial q_i \partial q_j}\right)_{Opt} \tag{3}$$

where $q_1 = \sqrt{m_1}\xi_1 = \sqrt{m_1}\Delta x_1, q_2 = \sqrt{m_1}\xi_2 = \sqrt{m_1}\Delta y_1$ and so on. $\mathbf{f}_{\mathrm{MWC}}$ is diagonalized, yielding a set of $3N$ eigenvectors and $3N$ eigenvalues.

The next step is to translate the center of mass to the origin, and determine the moments and products of inertia, with the goal of finding the matrix that diagonalize the moment of inertia tensor. Using this matrix we can find the vectors corresponding to the rotations and translations. Once these vectors are known, we know that the rest of the normal modes are vibrations. The center of mass $\mathbf{R}_{COM}$ is found in the usual way:

$$\mathbf{R}_{COM} = \frac{\sum_\alpha m_\alpha \mathbf{r}_\alpha}{\sum_\alpha m_\alpha} \tag{4}$$

where the sums are over the atoms, α. The origin is then shifted to the center of mass $\mathbf{r}_{COM_\alpha} = \mathbf{r}_\alpha - \mathbf{R}_{COM}$. Next we have to calculate the moments of inertia (the diagonal elements) and the products of inertia (off diagonal elements) of the moment of inertia tensor ($\mathbf{I}$).

$$\begin{aligned}\mathbf{I} &= \begin{Bmatrix} I_{xx} & I_{xy} & I_{xz} \\ I_{yx} & I_{yy} & I_{yz} \\ I_{zx} & I_{zy} & I_{zz} \end{Bmatrix} \\ &= \begin{Bmatrix} \sum_\alpha m_\alpha (y_\alpha^2 + z_\alpha^2) & -\sum_\alpha m_\alpha (x_\alpha y_\alpha) & -\sum_\alpha m_\alpha (x_\alpha z_\alpha) \\ -\sum_\alpha m_\alpha (y_\alpha x_\alpha) & \sum_\alpha m_\alpha (x_\alpha^2 + z_\alpha^2) & -\sum_\alpha m_\alpha (y_\alpha z_\alpha) \\ -\sum_\alpha m_\alpha (z_\alpha x_\alpha) & -\sum_\alpha m_\alpha (z_\alpha y_\alpha) & \sum_\alpha m_\alpha (x_\alpha^2 + x_\alpha^2) \end{Bmatrix}\end{aligned} \tag{5}$$

This symmetric matrix is diagonalized, yielding the principal moments (the eigenvalues $\mathbf{I}'$) and a 3×3 matrix ($\mathbf{X}$), which is made up of the normalized eigenvectors of ($\mathbf{I}$). The eigenvectors of the moment of inertia tensor are used to generate the vectors corresponding to translation and infinitesimal rotation of the molecular

Table 1
The optimized bond length (in Å) of C–C for different CNTs.

Aspect ratio (L/D)	Types of CNTs						
	(5, 0)	(6, 0)	(8, 0)	(10, 0)	(3, 3)	(4, 4)	(6, 6)
5.5	1.4219	1.4208	1.4185	1.4127	1.4219	1.4141	1.4101
9.8	1.4219	1.4181	1.4185	1.4143	1.4215	1.4154	1.4168
14.2	1.4212	1.4178	1.4152	1.4145	1.417	1.4184	1.4135
18.5	1.4219	1.4178	1.4185	1.4127	1.4218	1.4141	1.4157

Table 2
The optimized bond angle (in degrees) of C–C for different CNTs.

Aspect ratio (L/D)	Types of CNTs						
	(5, 0)	(6, 0)	(8, 0)	(10, 0)	(3, 3)	(4, 4)	(6, 6)
5.5	118.42	116.67	119.57	119.87	118.62	118.58	119.53
9.8	118.42	118.80	119.57	119.88	118.89	118.91	119.37
14.2	118.27	119.08	119.34	119.87	119.02	119.49	119.25
18.5	119.01	119.08	119.57	119.87	119.02	119.49	119.42

system. A Schmidt orthogonalization is used to generate $N_{vib} = 3N - 6$ remaining vectors, which are orthogonal to the six rotational and translational vectors. The result is a transformation matrix **D** which transforms from mass weighted Cartesian coordinates **q** to internal coordinates **S** = **Dq**, where rotation and translation have been separated out. Now that we have coordinates in the rotating and translating frame, we need to transform the Hessian, $\mathbf{f}_{MWC}$, to these new internal coordinates (INT) [33,34]. Only the N_{vib} coordinates corresponding to internal coordinates will be diagonalized, although the full 3*N* coordinates are used to transform the Hessian. The transformation is straightforward as follows:

$$\mathbf{f}_{INT} = \mathbf{D}^T \mathbf{f}_{MWC} \mathbf{D} \tag{6}$$

The $N_{vib} \times N_{vib}$ submatrix of $\mathbf{f}_{INT}$, which represents the force constants internal coordinates, is diagonalized yielding N_{vib} eigenvalues $\lambda = 4\pi^2\omega^2$, and N_{vib} eigenvectors. If we call the transformation matrix composed of the eigenvectors **L**, then we have

$$\mathbf{L}^T \mathbf{f}_{INT} \mathbf{L} = \mathbf{\Lambda} \tag{7}$$

where **Λ** is the diagonal matrix with eigenvalues λ_i. At this point, the eigenvalues need to be converted frequencies as

$$\omega_i = \sqrt{\frac{\lambda_i}{4\pi^2}} \tag{8}$$

3. Results and discussion

The resonant frequencies of SWCNT-based resonators depend on the tube diameter and length. The atomic structures of SWCNTs could also exert significant influence on their vibration behaviours. Thus, in this work, we analyze two groups of SWCNT resonators, i.e., four zigzag nanotubes (5, 0), (6, 0), (8, 0), (10, 0) and three armchair nanotubes (3, 3), (4, 4), (6, 6), with increasing diameters. The computational results of the first five vibrational frequencies of these zigzag and armchair SWCNTs are calculated in Figs. 1 and 2, respectively, as functions of the length-to-diameter aspect ratio. In this study, we computed our results using no restrains/free-free boundary conditions. For the comparison of the present approach with previous studies [35–38], we considered different boundary conditions. Our results are tabulated in Tables 3 and 4, which are in good agreement with previous studies.

3.1. Dependence of the aspect ratio and diameter

As shown in Figs. 1 and 2, for SWCNTs with the aspect ratio rising from around 5 to 20, the fundamental frequencies are in the ranges of 120–2300 GHz for the zigzag CNTs (5, 0), (6, 0), (8, 0), (10, 0). While for the armchair CNTs (3, 3), (4, 4), (6, 6), the variation of frequencies is between 85 and 2100 GHz. It may be noted from Refs. [31,39–41] that the resonant frequencies of SWCNTs obtained based on the present MM approach are close to, but lower than, those given by a structural mechanics approach. Specifically, the tendency of frequency to change with diameter and aspect ratio are generally in accordance with that given by these studies. The discrepancy is primarily a result of the different end constraints of SWCNTs considered in the present study and Refs. [31,40,41].

For both zigzag and armchair SWCNTs, the frequencies of all five modes are generally in decreasing trend when the aspect ratio increases from 5 to up to 20. The curves of frequency becomes steeper for the SWCNTs of smaller diameter. This shows that the dependence on the aspect ratio is stronger for the frequencies of thinner SWCNTs. In the meantime, it is also seen from Figs. 1 and 2 that, for a given aspect ratio the frequencies of SWCNTs always decline with rising diameters. To further examine this issue, we plotted the fundamental frequency as a function of tube diameter in Fig. 3. It is clear in Fig. 3 that the frequencies of small-diameter SWCNTs are always higher than the corresponding frequencies of large-diameter SWCNTs. This is especially so when the aspect ratio is relatively small. However, the effect of diameters diminishes when the aspect ratio grows. For example, in Fig. 3a, for armchair tubes with aspect ratio 5.43 the frequency decreases form 2154.61 to 1050.77 GHz when the diameter increases from 0.41

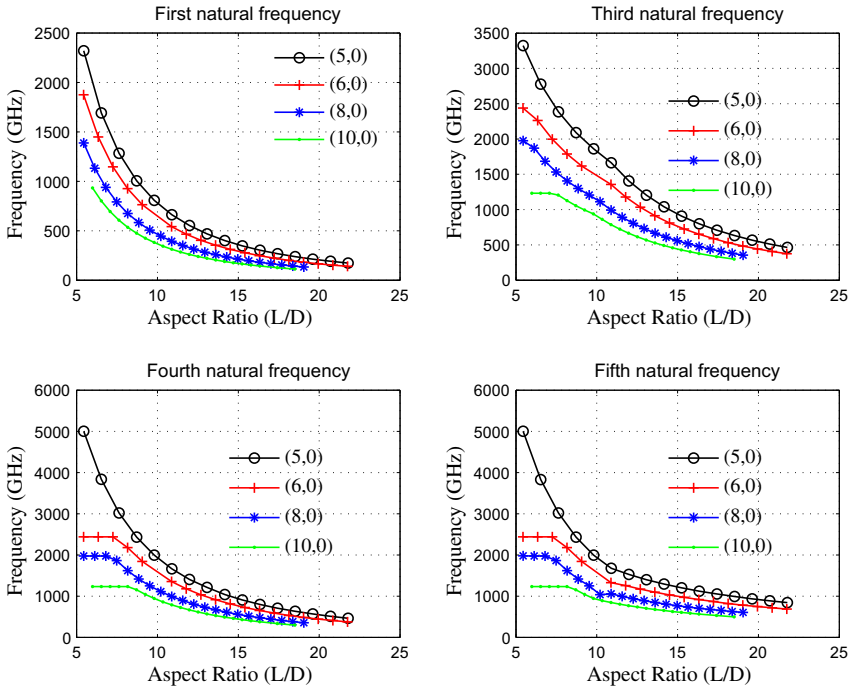

Fig. 1. First five vibrational frequencies of zigzag CNTs as a function of tube aspect ratio (*L*/*D*). First two modes are identical with different symmetric planes of flexural vibration. The 3rd mode corresponds to torsional vibration. The 4th and 5th modes correspond to higher flexural vibration.

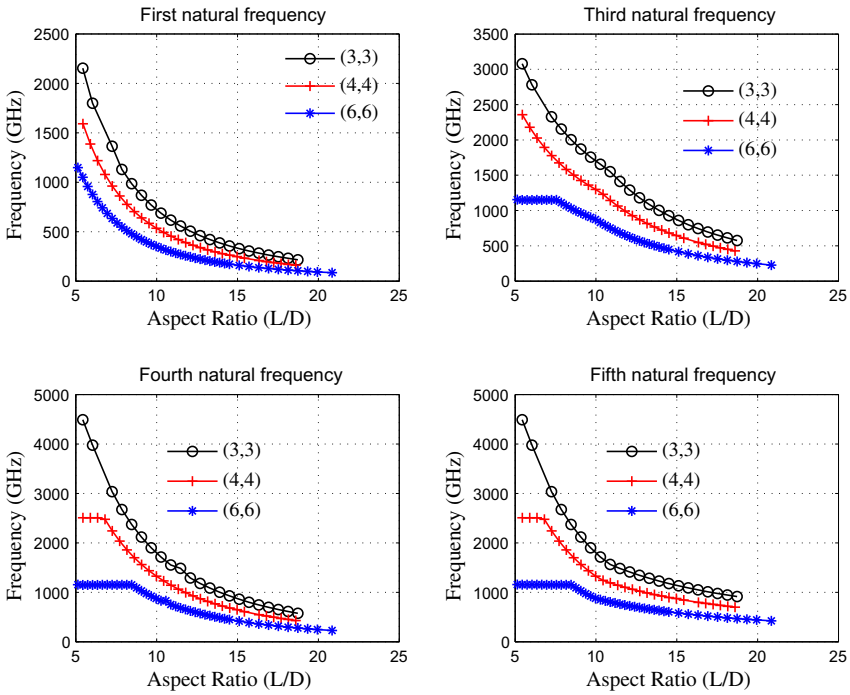

Fig. 2. First four vibrational frequencies of armchair CNTs as a function of tube aspect ratio (L/D). Similar to zigzag nanotubes, first two modes are identical with different symmetric planes of flexural vibration. The 3rd mode corresponds to torsional vibration. The 4th and 5th modes correspond to higher flexural vibration.

Table 3
Frequency of (5, 5) carbon nanotube in THz – Cantilever boundary condition.

Aspect ratio	Present analysis				Values from [35]			
	1st	2nd	3rd	4th	1st	2nd	3rd	4th
5.26	0.220	1.113	2.546	4.075	0.212	1.043	2.340	3.682
5.62	0.195	1.005	2.325	3.759	0.188	0.943	2.141	3.406
5.99	0.174	0.912	2.132	3.478	0.167	0.857	1.967	3.158
6.35	0.156	0.830	1.961	3.226	0.150	0.782	1.813	2.936
6.71	0.141	0.759	1.810	3.000	0.136	0.716	1.676	2.736
7.07	0.128	0.696	1.675	2.797	0.123	0.657	1.553	2.555
7.44	0.116	0.641	1.554	2.614	0.112	0.605	1.443	2.392
7.80	0.106	0.592	1.446	2.447	0.102	0.559	1.344	2.243
8.16	0.098	0.548	1.348	2.296	0.094	0.518	1.255	2.108
8.52	0.089	0.492	1.231	2.102	0.086	0.481	1.174	1.984

to 0.81 nm, while with the same diameter variation but larger aspect ratio 15.11 it only varies from 328.87 GHz to 158.89 GHz. Similar behaviour is also observed for zigzag tube in Fig. 3b. Thus we see that when the aspect ratio of SWCNTs grows from 5 to 20, the difference in frequency due to the variation of diameter decreases significantly whereas the ratio between the frequencies remains almost unchanged. This observation suggests that the influence of radial size on the vibration frequency of SWCNTs does not significantly change with increasing longitudinal size.

Here the decreasing frequencies with increasing aspect ratio and diameter observed in Figs. 1–3 can be attributed to the fact that SWCNTs of larger aspect ratio and diameter possess lower dynamic structural stiffness in both longitudinal and radial directions. In particular, for thinner SWCNTs of small-diameter their radial stiffness is strong. The frequency of such SWCNTs thus becomes more sensitive to their longitudinal rigidity, which finally leads to stronger effect of the aspect ratio for thin SWCNTs. On the other hand, for stocky tubes of small aspect ratio the longitudinal rigidity is high and thus the radial rigidity plays more significant role in altering the frequency of these SWCNTs. This explains the stronger diameter-dependence of frequency observed for shorter SWCNTs of smaller aspect ratio.

In addition, it is interesting to see form Figs. 1 and 2 that, while the frequency of SWCNTs usually tends to decrease with the increase of the aspect ratio, the frequencies of the 4th and 5th modes obtained for some SWCNTs of small aspect ratio (say 5–7) are almost a constant independent of the aspect ratio. To account for this observation we have studied the associated vibration modes of SWCNTs by using the MM model. An interesting circumferential vibration is achieved for the SWCNTs, where the bending and stretching in circumferential direction is predominant over the deformation in longitudinal directions (see Supplementary Materials). This is similar to the inextensional modes observed in [40] based on a similar MM model for zigzag SWCNTs, where deformation in longitudinal direction is negligible and thus the associated

Table 4
Frequency of carbon nanotube in cm^{-1} – Free-free boundary condition. Here ω^T: torsional frequency, ω^A: axial frequency, ω^R: Rayleigh frequency, ω^{RBM}: radial breathing frequency.

Tube (n, m)	Present analysis				Gupta et al. [36]				Lawler et al. [37]	Kurti et al. [38]
	ω^T	ω^A	ω^R	ω^{RBM}	ω^T	ω^A	ω^R	ω^{RBM}	ω^{RBM}	ω^{RBM}
(10, 0)	22.190	33.420	53.330	291.200	18.732	29.633	53.323	290.463	294	298
(16, 0)	13.535	18.671	28.878	182.023	11.633	18.329	27.781	181.747	177	188
(20, 0)	9.889	15.838	19.980	146.045	9.346	14.691	19.040	145.363	NA	150

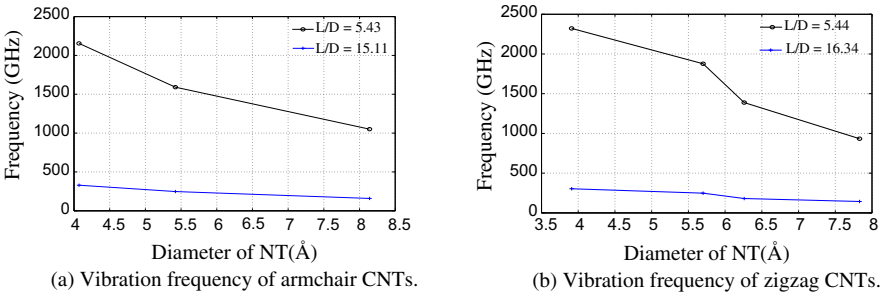

(a) Vibration frequency of armchair CNTs. (b) Vibration frequency of zigzag CNTs.

Fig. 3. Diameter dependence on vibration frequency of CNTs with different chirality.

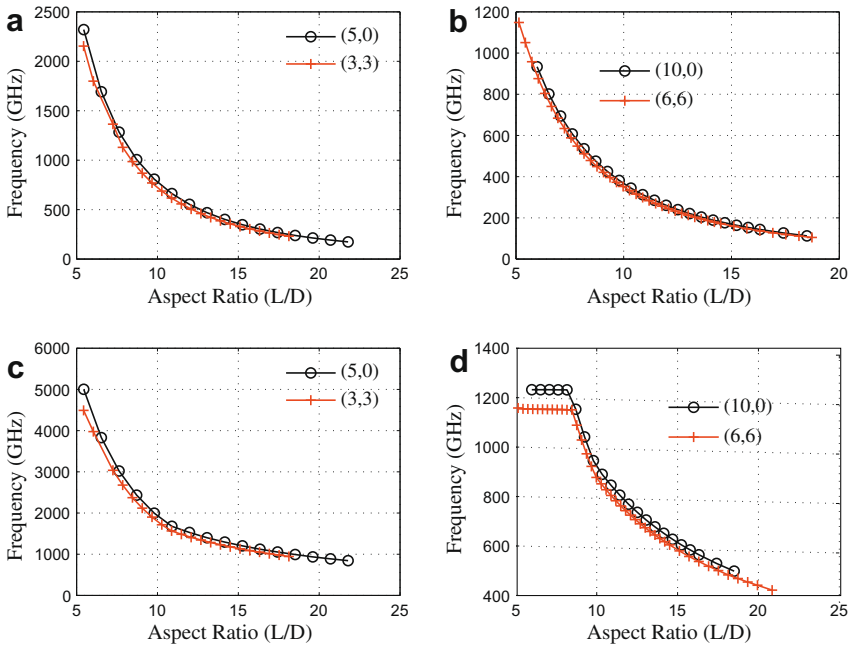

Fig. 4. Dependence of molecular structure on fundamental frequencies of CNTs. It is found that, natural frequencies of zigzag CNTs are higher compared to armchair CNTs. However, differences in frequencies diminishes with increase in aspect ratio.

frequency is independent of the aspect ratio. This indeed can also account for the aspect ratio independent frequencies shown in Figs. 1 and 2.

3.2. Effect of atomic structures

Next we examine the effect of atomic structures on the frequency of SWCNTs. To this end we plotted the fundamental frequency and the 5th frequency in Fig. 4, respectively, for both armchair and zigzag SWCNTs with the aspect ratio increasing from 5.5 to 18.5. Here zigzag tube (5, 0) and armchair tube (3, 3) compared in Fig. 4a and c have the diameter of around 0.4 nm, while tube (10, 0) and tube (6, 6) considered in Fig. 4b and d are of diameter around 0.8 nm. In Fig. 4a and b, it is shown that for the same diameter the fundamental frequencies of zigzag SWCNTs are always higher than those of armchair SWCNTs in the whole length of the aspect ratio studied here. The difference between the frequencies of the two types of SWCNTs, however, are not very large. The maximum relative difference calculated as $(\omega_{\text{zigzag}} - \omega_{\text{armchair}})/\omega_{\text{armchair}}$ is of the order of 8%. Such discrepancy of the frequency due to the change of atomic structures decreases with rising aspect ratio and turns out to be negligible when the aspect ratio is sufficiently large, say >15. For the 5th frequency considered in the present study we have observed that, in a wide range of the aspect ratio, the frequencies of zigzag and armchair tubes almost coincide with each other. For SWCNTs the difference of atomic structures can be measured by the change in their chiral angles, where the maximum value 30° is obtained when the armchair and zigzag structures are considered. Thus, it is easy to understand that the frequency difference shown in Fig. 4 represents the most significant effect of the atomic structures on the 1st and 5th vibration modes of SWCNTs. In view of these results it follows that the frequency of SWCNTs is primarily determined by their geometric sizes, i.e., diameter and the aspect ratio, but cannot be substantially changed due to the variation of their atomic structures. This finding demonstrates that the continuum models can indeed forms a good approximation for the vibration of SWCNTs with different atomic structures and the radius down to 0.34 nm. Specifically, the obtained results suggest that the accuracy of the continuum models can be further improved for the vibration of SWCNTs with larger radii and greater aspect ratios.

On the other hand, large discrepancy has been identified in Fig. 4d for the 5th frequency of tube (10, 0) and (6, 6) at the small aspect ratio 5–7, where the frequency is found to be insensitive to the change of the aspect ratio. As explained above, the frequency is associated with the circumferential models which is similar to the inextensional modes of zigzag tubes reported in [36]. For such a vibration mode of SWCNTs the effect of atomic structures is strong and thus cannot be negligible in analysis. This means that contin-

uum models will lead to large errors and thus beak down for the circumferential mode, which is consistent with the conclusion drawn in [36] for the inextensional modes. In [36], the breakdown of continuum models is explained as a result of the short wavelength of this mode in circumferential direction.

Another issue relevant to nanomechanical resonators is the vibrational mode associated with the frequencies. It is found that the 1st and 2nd modes are identical in all cases. But the plane of vibration is symmetric. For the illustration purpose, the modes of vibration of (5, 0) with aspect ratio 8.71 and (4, 4) with aspect ratio 7.26 are provided in the supporting documents along with frequency data for all cases. Using a MM3 potential field, Gupta et al. [36] observe a saturation of frequencies for low circumferential wave numbers in both zigzag and armchair SWCNTs with short aspect ratio. Our model show a similar behaviour, starting for (6, 6) tubes from the third natural frequency, and progressing to higher mode shape orders for the (4, 4) (Fig. 2).

4. Conclusions

The vibrational properties of two kinds of single-wall carbon nanotubes (zigzag and armchair) are studied in the present research. A molecular mechanics based approach is used for estimate the frequencies. In this study, we used the UFF force field model, wherein the force field parameters are estimated using general rules based only on the element, its hybridization, and its connectivity. Vibration of CNTs show features of decreasing frequencies with increase in aspect ratio. It is found that, natural frequencies of zigzag CNTs are higher compared to armchair CNTs. However, differences in frequencies diminishes with increase in aspect ratio. In view of results presented, it follows that the frequency of SWCNTs is primarily determined by their geometric sizes, i.e., diameter and the aspect ratio, but cannot be substantially changed due to the variation of their atomic structures.

Acknowledgements

RC acknowledges the support of Royal Society through the award of Newton International Fellowship. SA gratefully acknowledges the support of The Leverhulme Trust for the award of the Philip Leverhulme Prize.

Appendix A. Supplementary material

Supplementary data associated with this article can be found, in the online version, at doi:10.1016/j.commatsci.2010.03.020.

References

[1] S. Iijima, Nature 354 (1991) 56.
[2] R.F. Gibson, E.O. Ayorinde, Y.-F. Wen, Composites Science and Technology 67 (2007) 1.
[3] C.Y. Wang, Y.Y. Zhang, C.M. Wang, V.B.C. Tan, Journal of Nanoscience and Nanotechnology 7 (2007) 4221.
[4] R.H. Baughman, A.A. Zakhidov, W.A. de Heer, Science 297 (2002) 787.
[5] K.T. Lau, D. Hui, Composites Part B – Engineering 33 (2002) 263.
[6] C.Y. Li, T.W. Chou, Physical Review B 68 (2003).
[7] C.Y. Li, T.W. Chou, Applied Physics Letters 841 (2004) 12.
[8] J. Yoon, C.Q. Ru, A. Mioduchowski, Journal of Applied Mechanics – Transactions of the ASME 72 (2005) 10.
[9] F. Scarpa, S. Adhikari, Journal of Non-Crystalline Solids 354 (2008) 4151.
[10] M.A. Pimenta, A. Marucci, S.D.M. Brown, M.J. Matthews, A.M. Rao, P.C. Eklund, R.E. Smalley, G. Dresselhaus, M.S. Dresselhaus, Journal of Materials Research 13 (1998) 2396.
[11] S. Rols, A. Righi, L. Alvarez, E. Anglaret, R. Almairac, C. Journet, P. Bernier, J.L. Sauvajol, A.M. Benito, W.K. Maser, et al., European Physical Journal B 18 (2000) 201.
[12] H. Kuzmany, W. Plank, M. Hulman, C. Kramberger, A. Gruneis, T. Pichler, H. Peterlik, H. Kataura, Y. Achiba, European Physical Journal B 22 (2001) 307.
[13] Z.H. Yu, L.E. Brus, Journal of Physical Chemistry B 105 (2001) 6831.
[14] R.R. Bacsa, A. Peigney, C. Laurent, P. Puech, W.S. Bacsa, Physical Review B 65 (2002).
[15] N. Yao, V. Lordi, Journal of Applied Physics 84 (1998) 1939.
[16] C.E. Bottani, A.L. Bassi, M.G. Beghi, A. Podesta, P. Milani, A. Zakhidov, R. Baughman, D.A. Walters, R.E. Smalley, Physical Review B 67 (2003).
[17] D.S. Tang, Z.X. Bao, L.J. Wang, L.C. Chen, L.F. Sun, Z.Q. Liu, W.Y. Zhou, S.S. Xie, Journal of Physics and Chemistry of Solids 61 (2000) 1175.
[18] B. Babic, J. Furer, S. Sahoo, S. Farhangfar, C. Schonenberger, Nano Letters 3 (2003) 1577.
[19] R.A. Jishi, L. Venkataraman, M.S. Dresselhaus, G. Dresselhaus, Chemical Physics Letters 209 (1993) 77.
[20] J. Yu, R.K. Kalia, P. Vashishta, Journal of Chemical Physics 103 (1995) 6697.
[21] R. Saito, T. Takeya, T. Kimura, G. Dresselhaus, M.S. Dresselhaus, Physical Review B 57 (1998) 4145.
[22] D. Sanchez-Portal, E. Artacho, J.M. Soler, A. Rubio, P. Ordejon, Physical Review B 59 (1999) 12678.
[23] V.N. Popov, V.E. Van Doren, M. Balkanski, Physical Review B 61 (2000) 3078.
[24] V.P. Sokhan, D. Nicholson, N. Quirke, Journal of Chemical Physics 113 (2000) 2007.
[25] C.Y. Wang, C.Q. Ru, A. Mioduchowski, Journal of Applied Mechanics – Transactions of the ASME 71 (2004) 622.
[26] C.Y. Wang, C.Q. Ru, A. Mioduchowski, Journal of Applied Physics 97 (2005).
[27] C.Y. Wang, C.Q. Ru, A. Mioduchowski, Journal of Applied Physics 97 (2005).
[28] C.Y. Wang, C.Q. Ru, A. Mioduchowski, Physical Review B 72 (2005).
[29] S.K. Georgantzinos, N.K. Anifantis, Computational Materials Science 47 (2009) 168.
[30] T.W. Odom, J.L. Huang, P. Kim, C.M. Lieber, Nature 391 (1998) 62.
[31] C.Y. Li, T.W. Chou, International Journal of Solids and Structures 40 (2003) 2487.
[32] A.K. Rappe, C.J. Casewit, K.S. Colwell, W.A. Goddard, W.M. Skiff, Journal of the American Chemical Society 114 (1992) 10024.
[33] D.F. McIntosh, Theoretical Chemistry Accounts: Theory, Computation, and Modeling 125 (2010) 177.
[34] M.J. Frisch, G.W. Trucks, H.B. Schlegel, G.E. Scuseria, M.A. Robb, J.R. Cheeseman, G. Scalmani, V. Barone, B. Mennucci, G.A. Petersson, et al., Gaussian 09 Revision A.1.
[35] W.H. Duan, C.M. Wang, Y.Y. Zhang, Journal of Applied Physics 101 (2007).
[36] S.S. Gupta, F.G. Bosco, R.C. Batra, Journal of Applied Physics 106 (2009).
[37] H.M. Lawler, D. Areshkin, J.W. Mintmire, C.T. White, Physical Review B 72 (2005).
[38] J. Kurti, G. Kresse, H. Kuzmany, Physical Review B 58 (1998) R8869.
[39] M. Mir, A. Hosseini, G.H. Majzoobi, Computational Materials Science 43 (2008) 540.
[40] K. Hashemnia, M. Farid, R. Vatankhah, Computational Materials Science 47 (2009) 79.
[41] S.K. Georgantzinos, G.I. Giannopoulos, N.K. Anifantis, Computational Mechanics 43 (2009) 731.